Structural determinants of unexpected agonist activity in a retro-peptide analogue of the SDF-1α N-terminus

Pasquale Palladino[a,*], Barbara Tizzano[a], Carlo Pedone[a], Raffaele Ragone[b], Filomena Rossi[a], Gabriella Saviano[c], Teodorico Tancredi[d], Ettore Benedetti[a]

[a] *Dipartimento delle Scienze Biologiche, C.I.R.Pe.B., Università Federico II di Napoli and Istituto di Bioimmagini e Biostrutture, CNR, Via Mezzocannone 16, 80134 Napoli, Italy*
[b] *Dipartimento di Biochimica e Biofisica and CRISCEB, Seconda Università di Napoli, Via Costantinopoli 16, 80138 Napoli, Italy*
[c] *Dipartimento di Scienze e Tecnologie per l'Ambiente e il Territorio, Università degli Studi del Molise, Via De Gasperi, 86170 Isernia, Italy*
[d] *Istituto di Chimica Biomolecolare, CNR, Via Campi Flegrei 34, 80078 Pozzuoli, Italy*

Received 29 April 2005; revised 4 July 2005; accepted 25 July 2005

Available online 12 September 2005

Edited by Christian Griesinger

Abstract **We have synthesised two retro-peptide analogues of the stromal cell derived growth factor 1 (SDF-1α) segment known to be critical for CXCR4 receptor binding, corresponding to the sequences HSEFFRCPCRFFESH and HSEFFRGGG-RFFESH. We have assayed the ability of these peptides to activate extracellular signal-regulated kinase 1/2 phosphorylation in cells over expressing the SDF-1α receptor, finding that the first variant was able to serve as an agonist of CXCR4, whereas the second one was inactive. Finally, by comparing representative solution structures of the two peptides, we have found that the biological response of HSEFFRCPCRFFESH may be ascribed to a β-β-type turn motif centred on Phe[4]–Phe[5].**

Keywords: Chemokine; CXCR4; SDF-1α; NMR

1. Introduction

The homeostatic CXC chemokine stromal cell derived growth factor 1 (SDF-1α) is the only known endogenous agonist for CXCR4, a receptor highly expressed in human malignant melanoma, malignant breast tumours and metastases, also shown to be an HIV-1 co-receptor [1]. Binding and activation assays indicate that the 29–39 N-terminus fragment near the transmembrane region of CXCR4 is required for activation by SDF-1α, whereas the 1–28 amino terminus segment of CXCR4 is neither necessary nor sufficient for activation [2]. As concerns the SDF-1α, the N-terminal lysine (and, possibly, proline at position 2) residue(s) seems to be required for SDF-1α activity [3]. The RFFESH sequence, located in the loop region of SDF-1α at positions 12–17, is necessary for optimal binding, but not sufficient for receptor activation [3]. This sequence is involved in the initial docking step of a process leading the N-terminal residues KPVSLSYR at positions 1–8 to interact with the more buried receptor site. In a model proposed for binding of SDF-1α to CXCR4, dimeric SDF-1α first interacts with endothelial-cell-surface glycosaminoglycans and, thereafter, with dimeric CXCR4 receptor [4].

On this basis, we have modelled the SDF-1α/CXCR4 interaction by the 1–17 N-terminal segment of human SDF-1α (KPVSLSYR-CPC-RFFESH), SDF-1{1–17}, and the 29–39 fragment of CXCR4 (FREENANFNKI), CXCR4{29–39} [5], respectively, showing that these peptides bind with a dissociation constant (K_d) in the micromolar range. Aiming to inhibit the chemotactic response of the CXCR4 receptor, we have used SDF-1{1–17} as a template to further synthesise two N-terminal analogues of SDF-1α. Namely, we kept the sequence claimed to be responsible for binding to CXCR4 [3,5], RFFESH, and replaced the segment supposed to be indispensable for receptor activation [3], KPVSLSYR, with the RFFESH-derived retro-peptide, thus obtaining the analogue of sequence HSEFFR-CPC-RFFESH, SDF-1{H–H}. Moreover, we substituted the CPC moiety, which makes SDF-1α a CXC-type chemokine, with three glycines, thus obtaining the analogue corresponding to the sequence HSEFFR-GGG-RFFESH, SDF-1{HG_3H}. This work reports on the structure–activity relationships of these peptides.

2. Materials and methods

2.1. Peptide synthesis

The N-terminal analogues of SDF-1α, SDF-1{1–17}: KPVSLSYR-CPCRFFESH, SDF-1{H–H}: HSEFFRCPCRFFESH and SDF-1{HG_3H}: HSEFFRGGGRFFESH, were synthesised by standard Fmoc solid phase peptide synthesis, purified by RP-HPLC and characterised by MALDI-TOF mass spectrometry, as described elsewhere [5]. Concerning the CPC sequence in SDF-1{H–H}, we have verified that the cysteine thiol groups were in reduced form even after strong oxidising treatment.

2.2. NMR spectroscopy

Samples were prepared by dissolving the peptide in water (90/10 v/v H_2O/D_2O) up to a concentration of 2 mM. The pH was adjusted to 5.0 according to the conditions used in previous studies [6,7]. NMR spectra were acquired at 280 K using a 600 MHz Varian Inova spectrometer or a 500 MHz Bruker DRX spectrometer. ^1H–^{13}C spectrum (HSQC) [8] and ^1H TOCSY [9], NOESY [10] and double quantum filtered COSY [11] spectra were used for resonance assignments. NOESY

*Corresponding author. Fax: +390812534560.
E-mail address: palladin@chemistry.unina.it (P. Palladino).

Abbreviations: CALIBA, calibration of NOE distance constraints; DYANA, dynamics algorithm for NMR applications; ECL, enhanced chemiluminescence; ERK1/2, extracellular signal-regulated kinases 1/2; MOLMOL, MOLecule analysis and MOLecule display; SDF-1α, stromal cell derived growth factor 1; TSSA, torsion space simulated annealing

0014-5793/$30.00
doi:10.1016/j.febslet.2005.07.100

mixing times were set at 100, 200, 350, and 500 ms in order to determine NOE build-up rates, which were found to be linear up to 350 ms. 2D-TOCSY experiments were recorded with mixing times of 30 and 70 ms. Sequence specific assignment was obtained by the combined use of TOCSY and NOESY experiments, according to the standard procedure [12]. Chemical shift values are reported in Tables 1 and 2.

2.3. Structure calculations

Peak integrals were evaluated by use of NMRView, transferred to the program package dynamics algorithm for NMR applications (DYANA) 1.0.6 [13], and converted to upper distance limits by using the calibration of NOE distance constraints (CALIBA) module of DYANA. Distance constraints were then worked out by the GRIDSEARCH module (also implemented in DYANA) to generate a set of allowed dihedral angles. Structure calculation was carried out with the macro ANNEAL by torsion angle dynamics. Eighty structures were calculated by torsion space simulated annealing (TSSA), starting with a total of 10 000 MD steps and a default value of maximum temperature. The twenty best structures in terms of target function were subjected to cluster analysis by best fitting of backbone atoms of residues from Glu^{3} to Asp^{6} with the program MOLecule analysis and MOLecule display (MOLMOL) [14].

2.4. Western blot analysis

CXCR4 was expressed on human neuroepithelioma CHP100 cells, according to a previously reported procedure [15,16]. Blots were incubated for 1 h with 5% non-fat dry milk or 3% bovine serum albumin to block non-specific binding sites and then incubated with specific antibodies. The immunoreactivity was detected with a enhanced chemiluminescent substrate (ECL). Relative band intensity was evaluated by densitometry (Scan Jet 4c HP) and software analysis (Jandel, Sigma Gel).

3. Results

3.1. Sequential assignment and secondary structures

The TOCSY spectra show well resolved resonances for almost all residues. However, some overlap is observed for the peptide SDF-1{H–H} which exhibits identical β and aromatic protons chemical shifts for residues Phe^{5}, Phe^{11} and Phe^{12}. The chemical shifts corresponding to the backbone amidic and alpha protons for these residues are, on the other hand, not degenerate (see Table 1), allowing the unambiguous use of the related NOEs in structural calculations. The Cys^{7}–Pro^{8} peptide bond was found in trans configuration, as indicated by the small difference (ca. 5 ppm) of the ^{13}C chemical shifts between β- and γ-carbon atoms of the proline residue.

$^{3}J_{NH-CH}$ coupling constant values are in the range of multiple ϕ angle values for both peptides, and therefore are not included in structure calculations. Temperature coefficient analysis of NHs for both peptides indicates that all amide protons are exposed to solvent, in accordance with previous findings [6]. NOESY spectra show strong $d_{\alpha N(i,i+1)}$ and weak $d_{NN(i,i+1)}$ sequential effects for both peptides (see Fig. 1). As

Table 1
^{1}H chemical shift values for the peptide SDF-1{H–H}

AA	NH	αCH	βCH	γCH	δCH	Other
His^{1}		4.10	3.15			4H 7.14/2H 8.36
Ser^{2}	8.71	4.24	3.59			
Glu^{3}	8.56	4.06	1.58/1.66	1.93/2.00		
Phe^{4}	8.16	4.35	2.69/2.80			2,6H 6.9
Phe^{5}	7.97	4.26	2.7			2,6H 6.9
Arg^{6}	8.02	3.95	1.40/1.48	1.27	2.91	εNH 6.98
Cys^{7}	8.21	4.39	2.63/2.63			
Pro^{8}		4.16	1.67/2.04	1.78/1.78	3.53/3.55	
Cys^{9}	8.25	4.14	2.61/2.61			
Arg^{10}	8.24	3.99	1.39/1.39	1.18/1.18	2.87	εNH 6.92
Phe^{11}	7.99	4.2	2.7			2,6H 6.9
Phe^{12}	7.9	4.29	2.7			2,6H 6.9
Glu^{13}	8.01	4.05	1.65/1.77	2.1/2.1		
Ser^{14}	8.15	4.11	3.59			
His^{15}	7.98	4.27	2.87/3.02			4H 6.99/2H 8.28

Table 2
^{1}H chemical shift values of the peptide SDF-1{HG_3H}

AA	NH	αCH	βCH	γCH	δCH	Other
His^{1}		4.08	3.11			4H 7.13/2H 8.33
Ser^{2}	8.68	4.23	3.55/3.55			
Glu^{3}	8.47	4.07	1.60/1.65	1.97/1.97		
Phe^{4}	8.11	4.36	2.64/2.75			2,6H 6.89
Phe^{5}	8.04	4.30	2.71			2,6H 7.0/3,5H 6.9
Arg^{6}	8.02	3.92	1.26/1.26	1.38/1.51	2.85/2.85	εNH 6.92
Gly^{7}	7.65	3.61/3.61				
Gly^{8}	8.10	3.66/3.66				
Gly^{9}	8.10	3.64/3.64				
Arg^{10}	7.93	3.93	1.32/1.32	1.11/1.11	2.80	εNH 6.85
Phe^{11}	8.02	4.28	2.62/2.74			2,6H 6.87/3,5H 7.02
Phe^{12}	7.89	4.25	2.75/2.66			2,6H 6.90
Glu^{13}	7.95	4.04	1.61/1.74	2.1/2.1		
Ser^{14}	8.09	4.07	3.55/3.55			
His^{15}	7.99	4.28	2.84/3.00			4H 6.97/2H 8.27

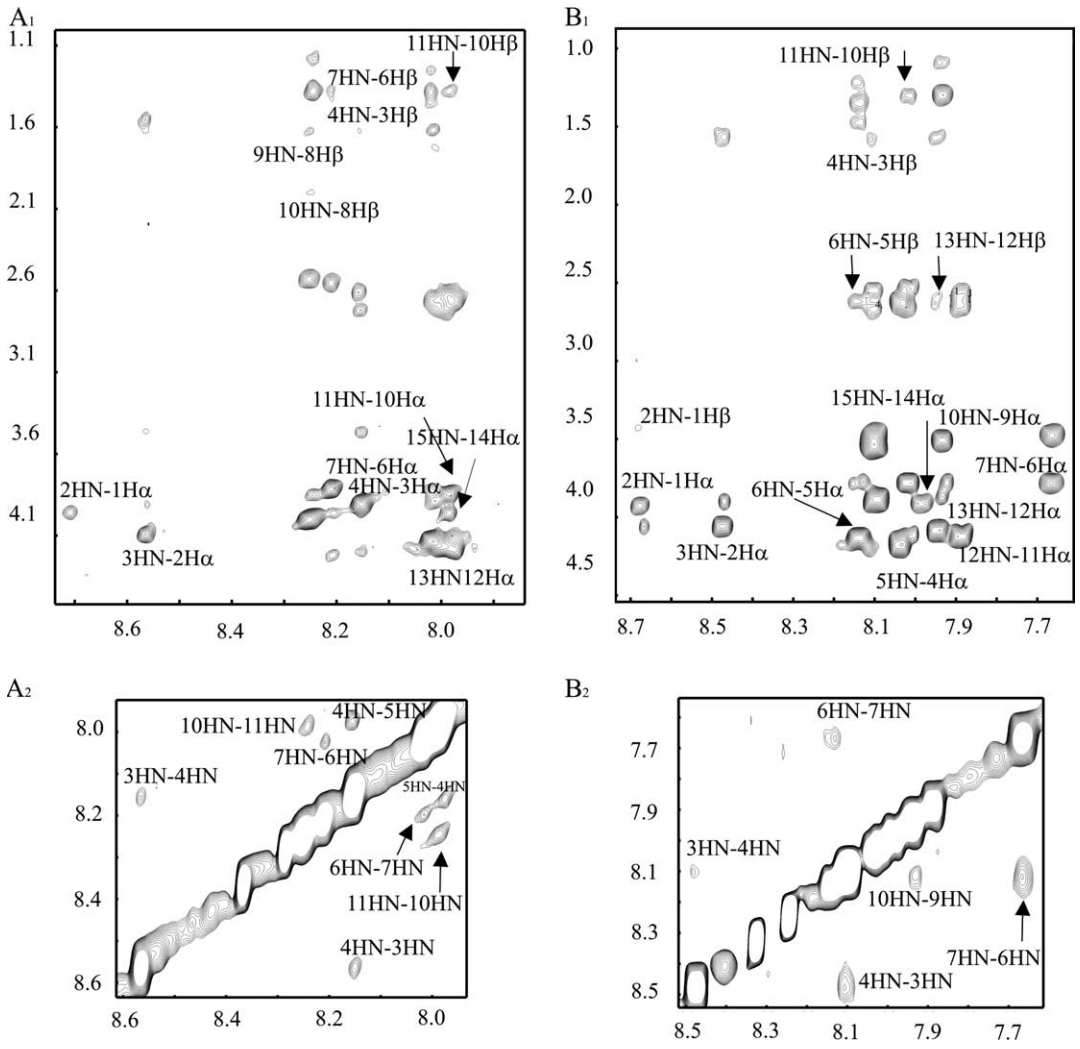

Fig. 1. Regions of 350-ms NOESY spectra. Panels A_1/A_2 (SDF-1{H–H}) and B_1/B_2 (SDF-1{HG_3H}) show the $d_{\alpha N}[i,i+1]$ and $d_{NN}[i,i+1]$ connectivities.

reported above, overlap of side chains proton resonances of Phe 5, 11 and 12 of peptide SDF-1{H–H} does not allow the unambiguous assignment of the NOE effects involving the side chain protons of these residues, and therefore they have not been included in the structural analysis. However, we have avoided problems arising from the massive overlap of signals by aligning peptides on the basis of their sequence identities and assigning HN–$HN_{(i,i+1)}$ NOEs according to the pattern previously found for SDF-1{1–17} [6], in which residues at positions 5–8 form a β-αR type turn:

SDF-1{1–17}	KPVSLSYR-CPC-RFFESH
SDF-1{H–H}	HSEFFR-CPC-RFFESH
SDF-1{HG_3H}	HSEFFR-GGG-RFFESH

Sequential and medium range NOEs for peptides SDF-1{H–H} and SDF-1{HG_3H} are summarised in Fig. 2A and B. From a preliminary analysis of all spectral parameters, the presence of both extended and folded regions of the backbone for both peptides was hypothesised. Observation of fairly strong $d_{\alpha N(i,i+1)}$ effects indicates the prevailing presence of extended structures, in agreement with the behaviour of chemical shifts, temperature coefficients and coupling constants. The presence of $d_{NN(i,i+1)}$ effects, however, shows that a folded structure (or a family of such structures) is also present and makes it possible to interpret the observed backbone NOEs for both SDF-1{H–H} and SDF-1{HG_3H} on the basis of a mixture of folded and extended conformers.

In analogy with previous work on SDF-1{1–17} [6], the d_{NN} effect between Phe^4 and Phe^5 in SDF-1{H–H} suggests the presence of a turn involving residues Glu^3, Phe^4, Phe^5 and Arg^6, with the two aromatic residues occupying the positions 2 and 3. However, it is not possible to classify definitely this turn as the β-αR type featured by SDF-1{1–17} [6], because the presence of a $d_{\alpha N}$ ($2 \rightarrow 4$) effect between Phe^4 and Arg^6 is ambiguous, due to overlapped resonances. d_{NN} connectivities are also observed between Glu^3 and Phe^4 as well as Arg^6 and Cys^7, suggesting a partial fold of the amino terminal part of the peptide. Moreover, even in our case, there is evidence of a second local structure involving the small sequence Arg^{10}–Phe^{11}. This structure may not be univocal, since it is based on a limited number of interatomic distances of the N-terminal residues of the sequence, but it is possible to test the validity by

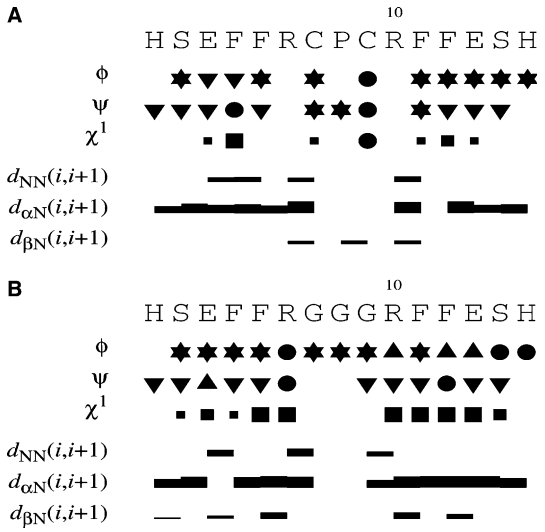

Fig. 2. Sequential and medium range NOE connectivities. Connectivities were derived from NOESY spectra at 350 ms mixing time for SDF-1{H–H} and SDF-1{HG_3H} (panels A and B, respectively). Backbone NOE connectivities are indicated by horizontal lines between residues, with thickness indicating their relative magnitude. The first three lines below the amino acid sequence represent torsion angle restraints for the backbone torsion angles ϕ and ψ, and for the side-chain torsion angle χ_1. For ϕ and ψ, a ▲ symbol indicates compatibility with an ideal α-helix or 3_{10}-helix; a ▼ symbol indicates compatibility with an ideal parallel or antiparallel β-strand; a ★ symbol encloses conformation of both α and β secondary structure types; and a ● symbol marks a restraint that excludes the torsion angle values of these regular secondary structure elements. Torsion angle restraints for χ_1 are depicted by filled squares of three different decreasing sizes, depending on whether they allow for one, two or all three of the staggered rotamer positions.

internal energy calculations and, most of all, by checking the consistency with biological activity.

3.2. Structure calculations and analysis

A total of 118 observed NOEs were used for structure calculations of SDF-1{H–H}. Distance restraints derived from intra-residue, sequential and medium range NOEs were introduced in SA torsion space calculation performed by DYANA package. The best twenty structures in terms of RMSD were selected from 80 structures sampled in TSSA calculations. An analogous procedure has been employed for calculations on SDF-1{HG_3H}.

Backbone clustering analysis for SDF-1{H–H} in the region 3–6 led to the identification of four structural families. The most populated one contains 13 structures with a backbone RMSD of 0.36 ± 0.14 Å for residues 3–6. Fig. 3 (top) illustrates, from residue 2 to 7, the bundle of conformers pertaining to the major subfamily of the SDF-1{H–H} peptide, with the best fitting of the sequence segment 3–6. A comparison between the canonical angles for a β-αR type turn with the angles of a representative structure for peptide SDF-1{H–H} shows a close similarity for all angles except for ψ of Phe^5, which suggests a β-β type turn (Table 3) [17]. The same cluster analysis was carried out for SDF-1{HG_3H}, leading to the identification of five structural families. Fig. 3 (bottom) shows the representative structure of the most populated family of SDF-1{HG_3H} for residues 2–7. Even in this case, the backbone best fitting was performed on the segment 3–6 (Table 4).

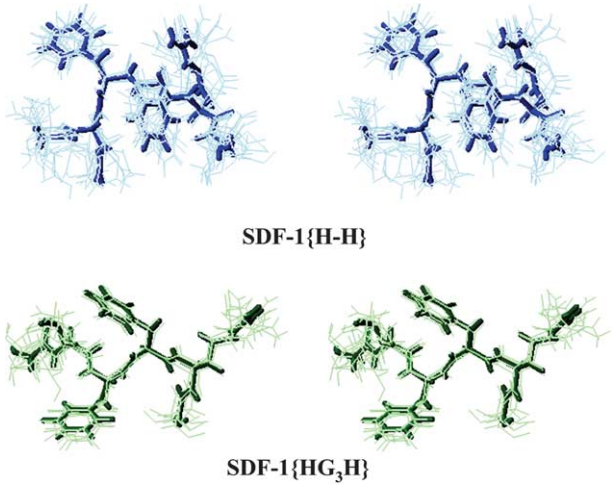

Fig. 3. Stereo view of the backbone clustering analysis for the region 3–6 of SDF-1{H–H} and SDF-1{HG_3H}. The mean structure of residues 2–7 from the major conformational subfamilies is indicated in bold for SDF-1{H–H} (top, blue) and SDF-1{HG_3H} (bottom, green).

3.3. Biological assays

Fig. 5 shows that an increased phosphorylation of extracellular signal-regulated kinases 1/2 (ERK1/2) occurred on stimulation of CHP100 cells with 125 nM SDF-1α (440 ± 26% of control values after 30 min). When cells were stimulated with either SDF-1{1–17} or SDF-1{H–H} for the same period, ERK1/2 phosphorylation was activated in a dose-dependent manner, reaching its maximal value at 250 nM for both compounds (190 ± 23% and 140 ± 13%, respectively; mean of three different experiments ± S.E.). Instead, the SDF-1{HG_3H} peptide was inactive.

4. Discussion

According to previous data [8,11], we have previously evaluated the affinity of the SDF-1α-based heptadecapeptide SDF-1{1–17} for the CXCR4-derived peptide CXCR4{29–39} [5]. We have then used SDF-1{1–17} as a template to synthesise two novel N-terminal analogues of SDF-1α, the pentadecapeptides SDF-1{H–H} and SDF-1{HG_3H}, both retaining the receptor binding motif RFFESH and lacking the N-terminal KPVSLSYR segment, which was substituted with the RFFESH-derived retro-peptide. Furthermore, in the SDF-1{HG_3H} sequence, the central CPC segment of SDF-1{H–H} was replaced by three glycines. By fluorimetric titrations (not shown), we have estimated that even these newly synthesised peptides bind to CXCR4{29–39}, as expected, with dissociation constants in the same micromolar range as that measured for SDF-1{1–17} [5]. Nevertheless, the solution structures of SDF-1{H–H} and SDF-1{HG_3H} at 280 K and pH 5.0, as determined by NMR spectroscopy and DYANA structure calculations, are quite different. A comparison between the N-terminal fragments including the residues at positions 2–7 underlines differences in both the structural fold of the backbone and the spatial disposition of side chains. Furthermore, SDF-1{H–H} does not show any antagonist activity toward the CXCR4 receptor, but behaves as an agonist, like SDF-1{1–17}, whereas SDF-1{HG_3H} is completely inactive.

Table 3
Angles and order parameters for the peptide SDF-1{H–H}[a]

Residue	ϕ	ϕS	ψ	ψS	χ_1	$\chi_1 S$
Ser^2			131.1 ± 35.0	0.836	−138.1 ± 71.7	0.561
Glu^3	−129.2 ± 102.0	0.359	79.7 ± 15.9	0.965	−47.5 ± 76.7	0.386
Phe^4	−111.9 ± 31.8	0.863	60.5 ± 20.1	0.944	−131.8 ± 10.3	0.985
Phe^5	−152.4 ± 22.2	0.933	161.7 ± 51.6	0.701	52.3 ± 15.1	0.968
Arg^6	−106.0 ± 74.0	0.555	83.0 ± 3.7	0.998	−41.9 ± 60.6	0.574
Cys^7	−113.4 ± 74.6	0.536			−132.0 ± 72.0	0.653

[a] ϕ, ψ, χ_1 and S values for residues 2–7, as computed from the structures of the major family identified by clustering residues 3–6.

Table 4
Angles and order parameters for the peptide SDF-1{HG$_3$H}[a]

Residue	ϕ	ϕS	ψ	ψS	χ_1	$\chi_1 S$
Ser^2			117.4 ± 21.4	0.941	150.4 ± 106.6	0.123
Glu^3	−124.0 ± 29.6	0.893	−54.1 ± 38.1	0.827	−99.6 ± 30.4	0.8
Phe^4	−24.2 ± 44.0	0.769	84.8 ± 13.8	0.975	−44.6 ± 59.6	0.621
Phe^5	−87.2 ± 2.7	0.999	149.6 ± 4.8	0.997	−46.8 ± 1.1	1.000
Arg^6	64.1 ± 0.1	1.000	67.9 ± 0.0	1.000	−60.5 ± 0.1	1.000
Gly^7	−99.6 ± 111.4	0.183				

[a] ϕ, ψ, χ_1 and S values for residues 2–7, as computed from the structures of the major family identified by clustering residues 3–6.

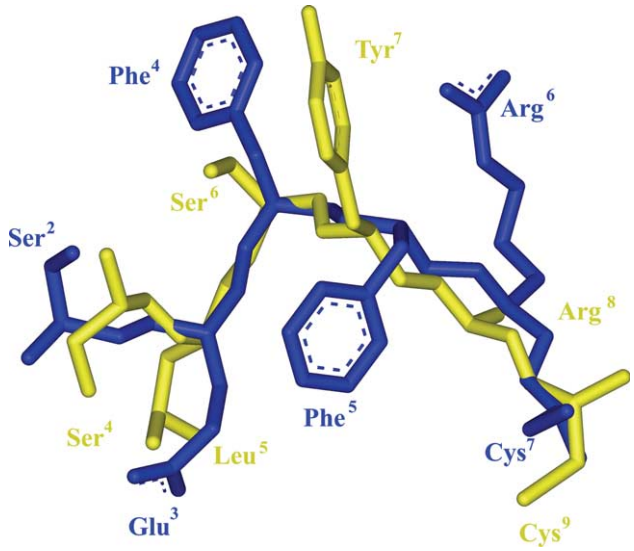

Fig. 4. Backbone superposition of SDF-1{H–H} and N-terminal region of SDF-1α. The solution structure (NMR, blue) of SDF-1{H–H} (residues 2–7) and the solid-state structure (X-ray, yellow) of the corresponding N-terminal region of SDF-1α (residues 4–9) are compared. The superposition is the best fitting of the region comprising residues 2–7.

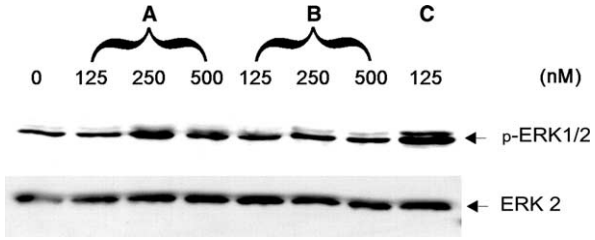

Fig. 5. Western blot analysis of ERK1/2 phosphorylation in human CHP100 neuroepithelioma cells. (A) SDF-1{1–17} (lanes 2–4); (B) SDF-1{H–H} (lanes 5–7); (C) SDF-1α (lane 8). Upper panel: anti phospho-ERK1/2. Lower panel: anti ERK2 as a control for equal protein loading.

By comparing the solution structures of the two analogues and determining the allowed conformer populations we have identified conformational differences responsible for the antipodal biological response. The assignment of HN–HN$_{(i,i+1)}$ connectivities according to those previously found for SDF-1{1–17} [6] entails that the SDF-1{H–H} structure displays a motif similar to a turn not stabilised by H-bonding and centred on the Phe^4–Phe^5 tract, closely resembling the N-terminal 4–9 fragment in the SDF-1α crystal structure (Fig. 4) [18].

Finally, it is worth noting that the biological behaviour of SDF-1{H–H} contrasts the view that wild-type Lys^1 and Pro^2 are necessary for determining the agonist activity of SDF-1α related peptides [3], but the recent identification of two novel agonists of the CXCR4 receptor [19], with a non-native 1–4 sequence in the N-terminal region, agrees with our conclusion. Nevertheless, the manner how the insertion of a bioactive peptide may affect the behaviour of the full-length chemokine is not plainly predictable. In conclusion, there is evidence that non-native sequences may be well involved in recognizing as well as activating the CXCR4 receptor, but comprehension of structural features underlying the chemokine biological response still needs in-depth studies (see Fig. 5).

References

[1] Feng, Y., Broder, C.C., Kennedy, P.E. and Berger, E.A. (1996) HIV-1 entry cofactor: functional cDNA cloning of a seven-transmembrane, G protein-coupled receptor. Science 272, 872–877.
[2] Doranz, B.J., Orsini, M.J., Turner, J.D., Hoffman, T.L., Berson, J.F., Hoxie, J.A., Peiper, S.C., Brass, L.F. and Doms, R.W. (1999) Identification of CXCR4 domains that support coreceptor and chemokine receptor functions. J. Virol. 73, 2752–2761.
[3] Crump, M.P., Gong, J.H., Loetscher, P., Rajarathnam, K., Amara, A., Arenzana-Seisdedos, F., Virelizier, J.L., Baggiolini, M., Sykes, B.D. and Clark-Lewis, I. (1997) Solution structure and basis for functional activity of stromal cell-derived factor-1; dissociation of CXCR4 activation from binding and inhibition of HIV-1. EMBO J. 16, 6996–7007.

[4] Babcock, G.J., Farzan, M. and Sodroski, J. (2003) Ligand-independent dimerization of CXCR4, a principal HIV-1 coreceptor. J. Biol. Chem. 278, 3378–3385.
[5] Palladino, P., Pedone, C., Ragone, R., Rossi, F., Saviano, M. and Benedetti, E. (2003) A simplified model of the binding interaction between stromal cell-derived factor-1 chemokine and CXC chemokine receptor 4. Protein Pept. Lett. 10, 133–138.
[6] Elisseeva, E.L., Slupsky, C.M., Crump, M.P., Clark-Lewis, I. and Sykes, B.D. (2000) NMR studies of active N-terminal peptides of stromal cell-derived factor-1. Structural basis for receptor binding. J. Biol. Chem. 275, 26799–26805.
[7] Booth, V., Slupsky, C.M., Clark-Lewis, I. and Sykes, B.D. (2003) Unmasking ligand binding motifs: identification of a chemokine receptor motif by NMR studies of antagonist peptides. J. Mol. Biol. 327, 329–334.
[8] Dorman, D.E. and Bovey, F.A. (1973) Carbon-13 magnetic resonance spectroscopy. The spectrum of proline in oligopeptides. J. Org. Chem. 38, 2379–2383.
[9] Bax, A. and Davis, D.G. (1985) MLEV-17-based two-dimensional homonuclear magnetization transfer spectroscopy. J. Magn. Res. 65, 355–360.
[10] Jeener, J., Meyer, B.H., Bachman, P. and Ernst, R.R. (1979) Investigation of exchange processes by two-dimensional NMR spectroscopy. J. Chem. Phys. 71, 4546–4553.
[11] Rance, M., Sörensen, O.W., Bodenhausen, G., Wagner, G., Ernst, R.R. and Wüthrich, K. (1983) Improved spectral resolution in COSY 1H NMR spectra of proteins via double quantum filtering. Biochem. Biophys. Res. Commun. 117, 479–485.
[12] Wüthrich, K. (1986) NMR of Proteins and Nucleic Acids, Wiley, New York.
[13] Güntert, P., Mumenthaler, C. and Wüthrich, K. (1997) Torsion angle dynamics for NMR structure calculation with the new program DYANA. J. Mol. Biol. 273, 283–298.
[14] Koradi, R., Billeter, M. and Wüthrich, K. (1996) MOLMOL: a program for display and analysis of macromolecular structures. J. Mol. Graph. 14, 51–55.
[15] Catani, M.V., Corasaniti, M.T., Navarra, M., Nisticò, G., Finazzi-Agrò, A. and Melino, G. (2000) gp120 induces cell death in human neuroblastoma cells through the CXCR4 and CCR5 chemokine receptors. J. Neurochem. 74, 2373–2379.
[16] Floridi, F., Trettel, F., Di Bartolomeo, S., Ciotti, M.T. and Limatola, C. (2003) Signalling pathways involved in the chemotactic activity of CXCL12 in cultured rat cerebellar neurons and CHP100 neuroepithelioma cells. J. Neuroimmunol. 135, 38–46.
[17] Wilmot, C.M. and Thornton, J.M. (1990) Beta-turns and their distortions: a proposed new nomenclature. Protein Eng. 3, 479–493.
[18] Dealwis, C., Fernandez, E.J., Thompson, D.A., Simon, R.J., Siani, M.A. and Lolis, E. (1998) Crystal structure of chemically synthesized [N33A] stromal cell-derived factor 1 alpha, a potent ligand for the HIV-1 fusin coreceptor. Proc. Natl. Acad. Sci. USA 95, 6941–6946.
[19] Sachpatzidis, A., Benton, B.K., Manfredi, J.P., Wang, H., Hamilton, A., Dohlman, H.G. and Lolis, E. (2003) Identification of allosteric peptide agonists of CXCR4. J. Biol. Chem. 278, 896–907.